

Wear Evaluation of Copper-Nickel-Aluminum Alloys under Extreme Conditions

Rene Guardian¹, Isai Rosales-Cadena^{1*}, Constanancio Diaz-Reyes¹, Juan Antonio Ruiz-Ochoa²

¹Center for Research in Engineering and Applied Sciences, Autonomous University of State of Morelos, Cuernavaca, Mexico

²Faculty of Sciences of the Enginy and Technology, UABC, Tijuana, Mexico

Email: *faye12@uaem.mx

How to cite this paper: Guardian, R., Rosales-Cadena, I., Diaz-Reyes, C. and Ruiz-Ochoa, J.A. (2023) Wear Evaluation of Copper-Nickel-Aluminum Alloys under Extreme Conditions. *Journal of Minerals and Materials Characterization and Engineering*, 11, 16-26.

<https://doi.org/10.4236/jmmce.2023.111002>

Received: November 18, 2022

Accepted: December 27, 2022

Published: December 30, 2022

Copyright © 2023 by author(s) and Scientific Research Publishing Inc. This work is licensed under the Creative Commons Attribution International License (CC BY 4.0).

<http://creativecommons.org/licenses/by/4.0/>



Open Access

Abstract

Cu-Ni-Al alloys at different concentrations were obtained using a high frequency induction melting unit, keeping a balance in the nominal compositions. Light alloys are important to be used in industrial applications. Aluminum additions result in a positive hardness increment of the ternary alloys in comparison with the binary Cu-Ni alloys. Generalized wear mechanisms of the alloys with low aluminum content are basically type abrasive, while samples with 5 and 10 at.% Al present an oxidative-adhesive wear mechanism. Wear results have indicated that aluminum addition affects positively the wear resistance, mainly in samples with high aluminum content product of the creation during the test of different oxides corresponding to the elements present in the alloys.

Keywords

Copper Nickel Alloys, Hardness, Mechanical Properties, Heat Treatment

1. Introduction

Strengthened alloys with enhanced mechanical and physical properties for specific applications are required for energy generation; copper-nickel based alloys may satisfy this requirement. Copper based alloys can be alloyed with a wide range of metals [1]; for this reason, they are considered as important alloys for applications in different specialized areas. It is well known that binary alloys may present some mechanical limitations; then it is necessary to introduce a third element; in this manner, many authors [2] [3] have developed investigations and reported the elements addition effect in the binary copper-nickel system, investigating their effect on the mechanical-microstructural behavior [4] [5] [6]. In copper-nickel alloys, ductility is attributed principally to the presence of differ-

ent copper phases [7] [8] [9], so that main applications are developed in mechanical assemblies, heat exchangers and intercoolers, among others.

On the other hand, nickel has been industrially used mainly to improve mechanical properties in nickel based super-alloys, and also extensive research has been developed related with its corrosion resistance in several environments [10]-[16]. Density in structural materials always has been an important factor to be taken into account for design and fabrication of different components. In this direction, it has been reported that Cu-Ni binary alloys present some limitations due to its relative high density [17]; therefore, aluminum addition may be an option to obtain improved mechanical and physical properties. Therefore, the purpose of this work is to generate the knowledge about the influence of the aluminum addition on the mechanical properties of the Cu-Ni and Cu-Ni-Al taking in consideration a substitutional mechanism.

2. Experimental Procedure

The alloys were obtained using high purity elements (99.99%) melted directly in a quartz crucible, using an induction power unit under vacuum atmosphere (10^{-3} torrs). **Table 1** presents the alloy designation taking in consideration the nominal compositions. Samples were heated up to 600°C and then water quenched, after that, annealing heat treatment was performed at 300°C for 180 minutes; metallographic polishing was developed by polishing the surface with paer grinding up to 1200 grade, after that, samples were polished using diamond paste $0.3\ \mu\text{m}$ and resultant samples were etched (immersed 15 s) with 5 g $\text{Fe}(\text{NO}_3)_3$, 25 ml HCl and 70 ml of deionized water. Wear specimens were cut from bars, with a dimension of $5 \times 5 \times 15$ mm.

Hardness measurements were carried out in a Microhardness tester LECO LM300AT, with 0.2 kg load and 15 s holding time. A conventional pin-on disk wear system was employed to evaluate the wear behavior of the pin samples at constant disk rotation of 200 rpm. The pin samples were worn against AISI 410 martensitic stainless steel as counterpart with a hardness of 45 HRC. The applied normal loads over the pin samples were 2.4 and 4.8 N. The resultant worn surfaces of the specimens were observed in a scanning electron microscope (SEM) equipped with an energy dispersive spectroscopy (EDS) system for determination of the oxygen percentages on the worn surfaces. Wear evaluations were

Table 1. Alloy designation taking in consideration the nominal compositions for the Cu-Ni-Al alloys and hardness values.

| Alloy Designation | Nominal Composition [at. %] | | | Hardness [kg/mm ²] |
|-------------------|-----------------------------|----|----|--------------------------------|
| | Cu | Ni | Al | |
| AB (binary alloy) | 90 | 10 | -- | 52 ± 8 |
| AT5 | 75 | 20 | 5 | 250 ± 10 |
| AT10 | 70 | 20 | 10 | 360 ± 5 |

carried out under zero lubrication.

3. Results and Discussions

Microstructure

In **Figure 1**, it can be observed the microstructure of the sample without aluminum addition, where it is observed an orderly growth of grains with an average grain size of 20 μm , *i.e.* coarse dendrite grains were developed as a result of continuous grain growth during solidification [2] also there are the apparition of precipitates (marked by arrows) distributed in homogeneous way over the entire surface but preferentially segregated along the grain boundaries, being its average size of 60 nm. This observed microstructure based in precipitation mechanism is product of the heat treatment applied [4] which was the purpose of the present work to improve the material performance.

The microstructure of the surface sample with 5 at.% Al is shown in **Figure 2**, where can be observed structure changes in comparison with the un alloyed sample due to the incorporation of the aluminum inner the Cu-Al structure which possesses an alpha face-centered cubic crystal structure [2], developing mostly equiaxed grains. It is important to note that precipitates are present preferentially in the grain boundaries, surrounding the dendritic structure, this fact it is important to be considered since this precipitation inhibit the dendritic growth. The composition of the observed precipitates is basically copper in major proportion with less nickel amount as can be observed in **Figure 3**.

Figure 3 shows the microstructure of sample with 10 at.% Al, where it is observed an α -phase dendritic morphology with eutectic structure in Cu-Ni matrix. Moderate precipitation is observed in this sample as was expected due to the aging treatment, inset in figure are the qualitative microanalyses in matrix as well in dendritic zones, it can be seen that the major nickel concentration is in

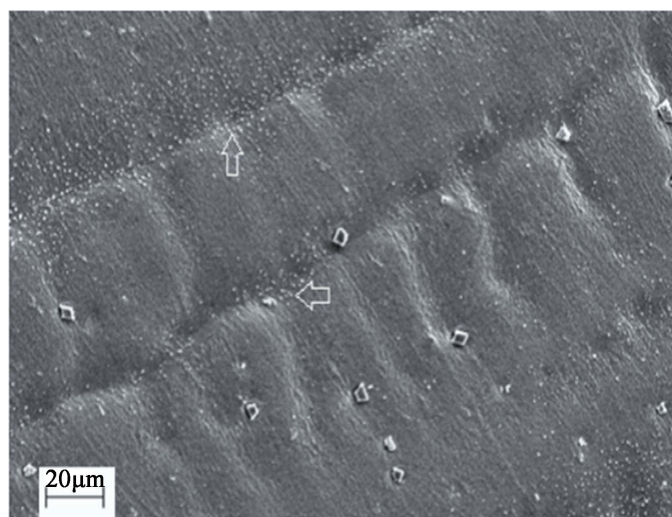


Figure 1. Microstructure of sample without aluminum additions, showing with arrows the presence of small precipitates nucleated during solidification.

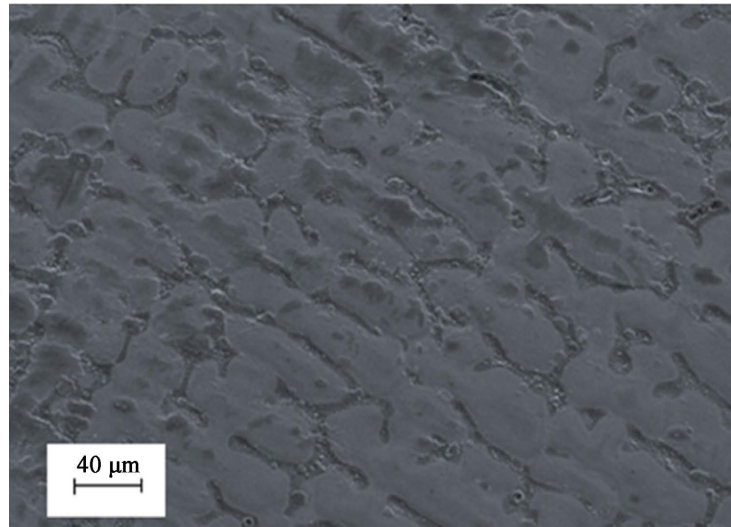


Figure 2. Microstructure of sample with 5 at.% aluminum additions, showing a dendritic structure with precipitates along the interdendritic regions.

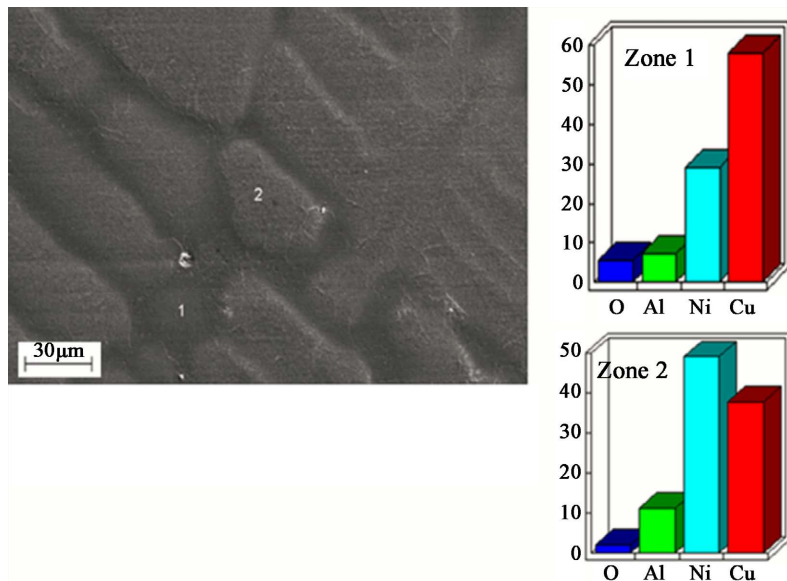


Figure 3. Microstructure of sample with 10 at.% aluminum additions, showing precipitates covering the full surface, qualitative microanalyses shown the chemical composition in both zones.

the inter-dendritic zone while a copper rich zone corresponds to the dendritic zone, these results suggest that the observed precipitates found around of dendritic zones are mainly nickel based precipitates [4].

4. Mechanical characterization

4.1. Hardness Test

Because the hardness of a material can be correlated with its wear resistance due to several factors, then, it is important to evaluate the intrinsic hardness of the material to know the probable operating |wear mechanism. In **Table 1**, it is pre-

sented the hardness values for the tested samples with different aluminum addition, namely 0, 5 and 10 at. % Al, where it is noticeable for samples without aluminum addition (AB), the hardness obtained is lower in comparison with the hardness of the ternary AT5 alloy in approximately five times which gets a hardness value of 260 kg/mm², while sample AT10 alloy increases its resistance value in approximately 350 kg/mm². Analyzing the aluminum addition effect, it is observed that binary alloy AB present the lower value in comparison with alloyed samples *i.e.* AT5 and AT10 present a noticeable hardness increment, this effect it is attributed (from a crystallographic point of view) to the lattice distortion by the incorporation of aluminum atoms, therefore low plastic deformation is reached when dislocation movement is partially inhibited by the existence of obstacles (misalignments planes) in the lattice, therefore a hardening effect is generated in the alloys. Similar statement has been established in Cu-Ni-Si alloys with a similar condition [8].

4.2. Wear Behavior

In **Figure 4**, it is presented the curves of the weight losses against sliding distance for the binary sample without heat treatment with a 2.4 N load. It is observed that for the first 800 meters there are no considerable weight losses for the alloyed samples, after this distance it is observed that sample with 5 at.% Al gradually lose weight until the test is over, while an abrupt mass detachment in sample with 10 at.% Al is observed at the same distance, presumably generated for the accumulation of aluminum oxides on the worn surface that were depicted after a saturation of these oxides, but a new oxide layer is created immediately on the surface in contact, thus it is observed that the operative wear mechanism for these samples is adhesive-oxidative. On the other hand unalloyed

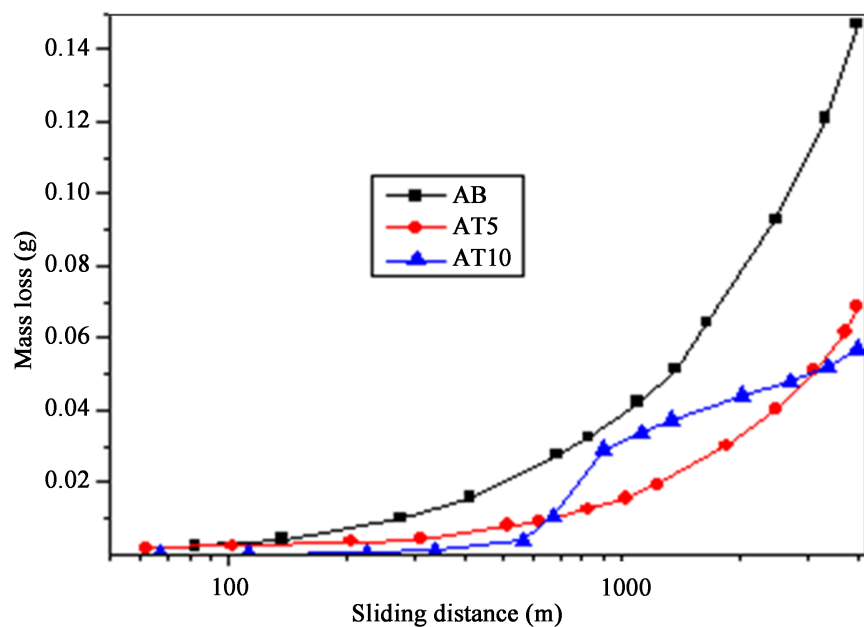


Figure 4. Plot of the weight losses versus sliding distance for samples with 2.4 N load.

sample presents a high wear losses regime observed after two hundred meters without the apparent oxide layer formation, This phenomena (increment of the slope) occurs due to the sudden depletion of the oxide layer formed due to the local heating between surface for this alloy the operative wear mechanism is abrasive type.

In **Figure 5**, it is observed the plot with the wear curves of samples with 4.8 N load, it is notorious that sample with 5 at.% Al presents a constant behavior without apparent weigh losses during the first five hundred meters followed by a slightly weight loose to later form a plateau, in this zone it is generated a oxide layer between surfaces in contact inhibiting the weight losses, after that the oxide layer thickness increases and it is detached spontaneously, then, the wear process start again. If the conditions or parameters remain constant, the process can by cyclic until the test is finished this occurs due to the influence of the aluminum that react with the oxygen present in the atmosphere and the elevated temperature generated by the friction during the test. The operating mechanism for this worn sample is totally of oxidative-adhesive. For the case of sample with 10 at.%Al, it is observed that the weight losses is gradual as the sliding distance increases, starting after the two hundred meters, perhaps due to the constant oxide formation between the surface sample and the counterpart, thus the oxide created acts as a lubricant but without enough adhesion on both surfaces, this result indicates that the operating mechanism is exclusively oxidative. On the other hand the wear curve for the unalloyed sample describes an exponential behavior which means an accelerated weight loss regime as is observed in the plot, in this case the sample it is worn without the plateau formation because there are no the conditions to create a protective oxide layer due to the precipitates on the surface sample that are detached and work in the system as abrasive particles.

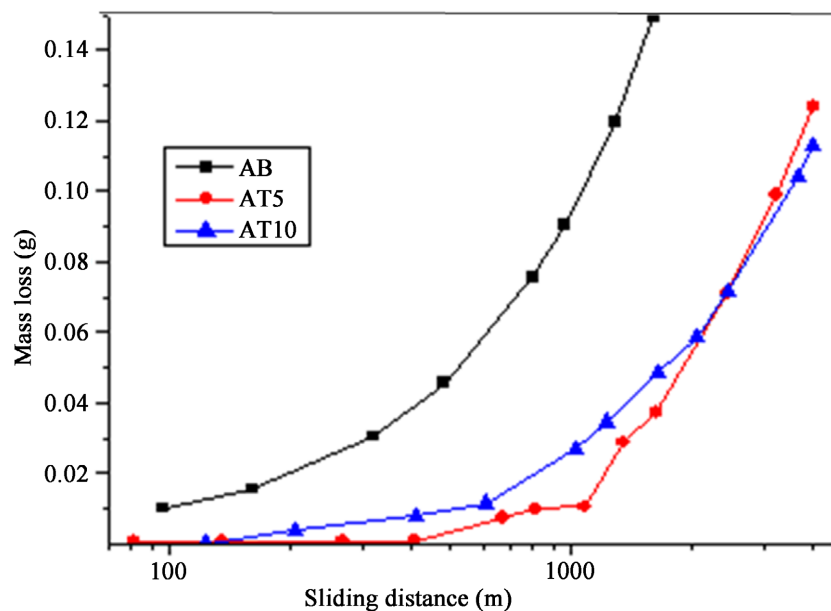


Figure 5. Plot of the weight losses versus sliding distance for samples with 4.8 N load.

Specifically for the AT5 curve which is not smooth those of AB and AT10 the interaction of the debris detached that acts as abrasive particle, then the sudden weight losses happen along the test in a no localized way, that means that the weight losses happen in generalized way, probably due to the scratches produced for the relative movement between the sample and the counterpart. The high values of weight losses observed in the plot, indicate an operating wear mechanism abrasive type.

In **Figures 6-8** are shown the SEM micrographs of wear tracks in surface samples with 0, 5, 10 at.% Al respectively after the test. In **Figure 6** can be observed the worn surface of the unalloyed sample, the total surface area is covered with scratches and grooves, product of the detached particles mainly from the surface sample against the counterpart, since the hardness of the counterpart is five times higher in comparison with this sample plus the effect of the applied load produced a catastrophic surface damage. Therefore, in these surfaces where there are no enough time and temperature to develop an oxide layer between the contact surfaces due to the constant detachment of sharp debris, being the operative wear mechanism is totally abrasive.

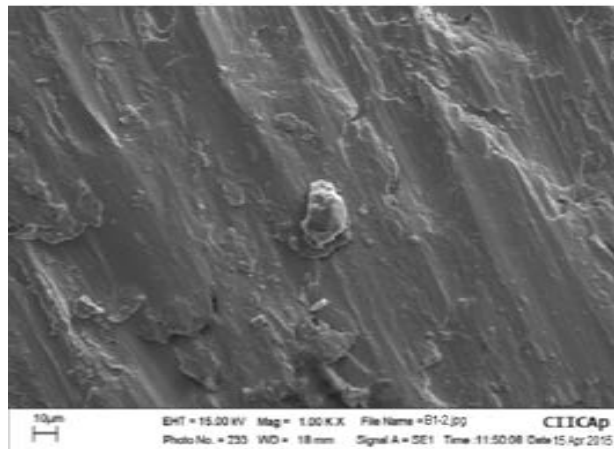


Figure 6. SEM image of the worn surface from sample with 0 at.% Al.

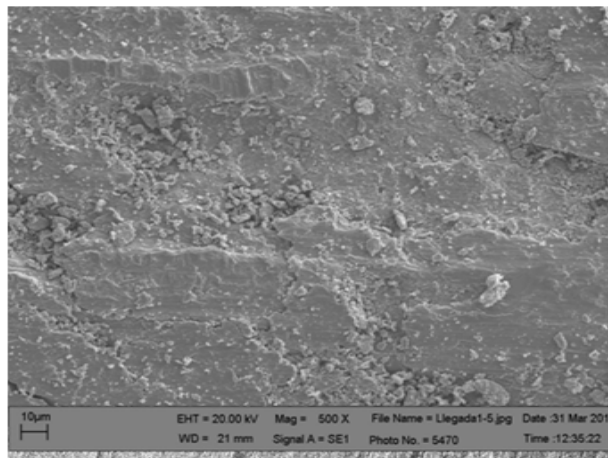


Figure 7. SEM image of the worn surface from sample with 5 at.% Al.

Figure 7 shows the worn surface of the sample with 5 at. % Al, where it is observed a generalized oxidized surface with few scratches along the sliding surface. Oxides generation by heating can be produced via higher friction rates due to the constant contact-movement between pin and counterpart, thereby as a result of such interaction, an oxidation reaction is developed with the presence of continuous oxide layer, then, the operating wear mechanism for this sample is oxidative-adhesive type.

In **Figure 8** is observed that surface sample with 10 at. % Al, few oxidation areas were detected generated by this friction phenomenon, which is attributed to the relative movement and the hardness difference between the counterpart (AISI-410) and the tested sample. In general, the oxide film has been principally formed on the worn surface sample; in this case, wear surface tracks that come from detached debris, are relatively low. In some areas of the wear surface, the produced layer presents micro cracks produced due to the internal stresses as consequence of the high regime of continuous contact, so that detachment of abrasive particles is produced [10] [11]; this fact, in some periods of sliding distance, tend to decrease the formation of the protective oxide layer, suggesting that the contact between the surfaces may generate a moderate friction rate. Thus the operating wear mechanism is a mixed mode between oxidative and abrasive.

4.2.1. Wear Factor Analysis

The calculation of the wear factor in worn samples under different conditions is an important issue to be analyzed to determine the relationship between the material detached from the surface sample in a specific distance or in a given time, taking in consideration tribological parameters such as: applied load, speed rotation of counterpart and lubrication. In **Figure 9** are observed the results obtained from the calculation of the wear factor from the wear curves formerly described. The plot shows the wear factor values for samples worn with a load of 2.4 N, where it is observed that all samples heat treated present the lower value

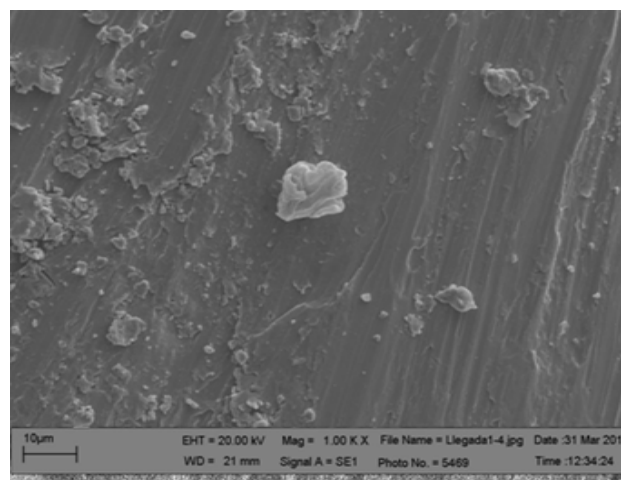


Figure 8. SEM image of the worn surface from sample with 10 at.% Al.

in their wear factor, that means that heat treatment produces an structural homogenization in samples and therefore an internal stress relief [18], this fact produces a decrease the wear factor in approximately 40 percent respect to the untreated samples.

For the case of samples worn with higher load, namely 4.8 N it is observed in **Figure 10** a noticeable increment in the wear factor value in samples unalloyed and without heat treatment of at least two times respect with the sample heat

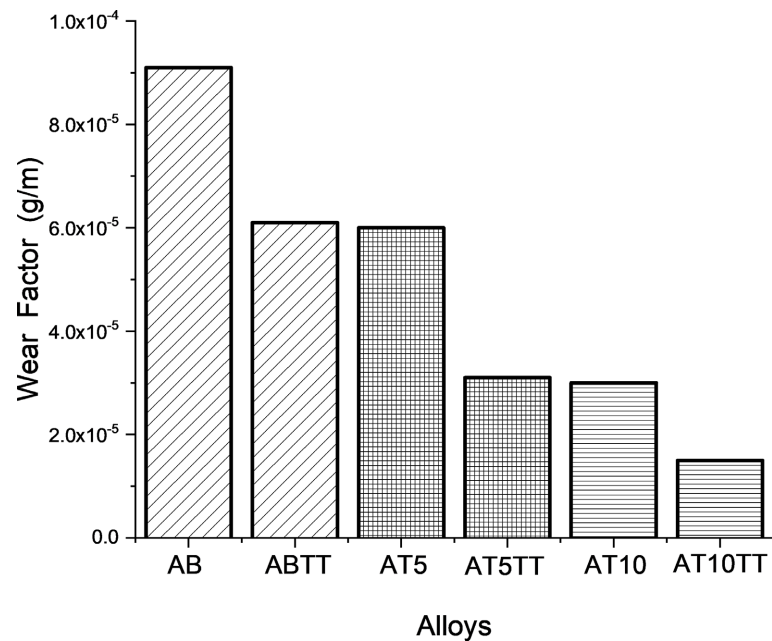


Figure 9. Values of wear factor calculated from curves of the worn samples with 2.4 N load.

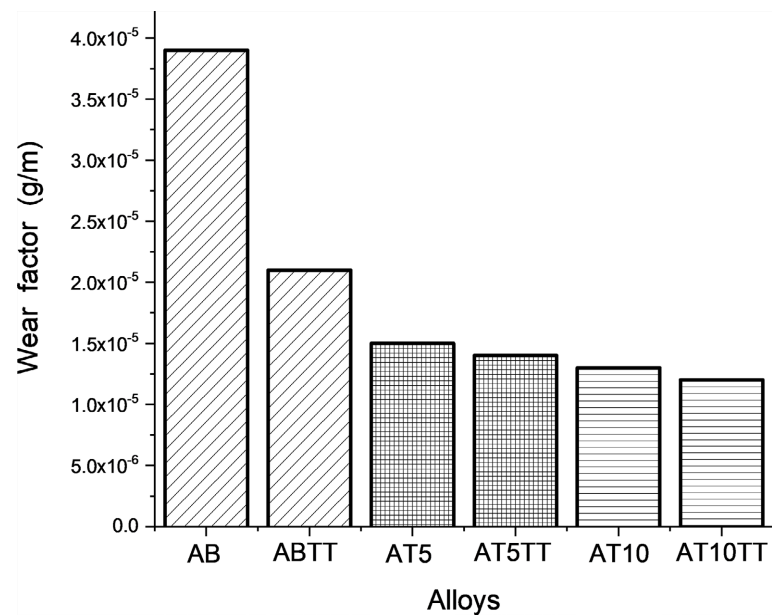


Figure 10. Values of wear factor calculated from curves of the worn samples with 4.8 N load.

treated and at least three times respect with the alloyed samples, this result represent a considerable improvement in wear resistance of the samples with aluminum addition, about it, is important to note that samples with 5 and 10 at.% Al, shown similar behavior in their wear factor values, indicating that low aluminum additions [18] may create also a protect oxide layer that improve the wear resistance.

5. Conclusion

Copper nickel alloys with aluminum additions were synthesized successfully, samples were heat treated and dendritic structure was obtained. Hardness evaluation has shown that heat treatment as well as aluminum addition improves their value approximately two times in comparison with the unalloyed sample. Wear results showed that improved wear resistance can be attributed to the formation of an oxide layer constituted with copper and aluminum which acts as a lubricant interphase. In general, results indicated that the alloy with 10 Al at.% is the most promissory to be used in applications with relative movement such as steam turbines bearings.

Acknowledgements

Authors are thankful with A. Aguilar for helpful support in mechanical characterization. This project was partially supported by PRODEP under grand PTC-074.

Conflicts of Interest

The authors declare no conflicts of interest regarding the publication of this paper.

References

- [1] Ricks, R.A., Howell, P.R. and Honeycombe, R.W.K. (1980) Formation of Supersaturated Ferrite during Decomposition of Austenite in Iron-Copper and Iron-Copper-Nickel Alloys. *Metal Science*, **14**, 562-568. <https://doi.org/10.1179/030634580790426229>
- [2] Lei, Q., Li, Z., Dai, C., Wang, J., Chen, X., Xie, J.M. and Chen, D.L. (2013) Effect of Aluminum on Microstructure and Property of Cu-Ni-Si Alloys. *Materials Science and Engineering: A*, **572**, 65-74. <https://doi.org/10.1016/j.msea.2013.02.024>
- [3] Schneider, M.S., Kad, B., Kalantar, D.H., Remington, B.A., Kenik, E., Jarmakani, H. and Meyers, M.A. (2005) Laser Shock Compression of Copper and Copper-Aluminum Alloys. *International Journal of Impact Engineering*, **32**, 473-507. <https://doi.org/10.1016/j.ijimpeng.2005.05.010>
- [4] Watanabe, K., Hashiba, M. and Yamashina, T. (1976) A Quantitative Analysis of Surface Segregation and In-Depth Profile of Copper-Nickel Alloys. *Surface Science*, **61**, 483-490. [https://doi.org/10.1016/0039-6028\(76\)90060-1](https://doi.org/10.1016/0039-6028(76)90060-1)
- [5] McFadden, S.X., Mishra, R.S., Valiev, R.Z., Zhilyaev, A.P. and Mukherjee, A.K. (1999) Low-Temperature Superplasticity in Nanostructured Nickel and Metal Alloys. *Nature*, **398**, 684. <https://doi.org/10.1038/19486>
- [6] Brandstetter, S., Zhang, K., Escudro, A., Weertman, J.R. and Van Swygenhoven, H.

- (2008) Grain Coarsening during Compression of Bulk Nanocrystalline Nickel and Copper. *Scripta Materialia*, **58**, 61-64. <https://doi.org/10.1016/j.scriptamat.2007.08.042>
- [7] Zhang, Y., Ping, L.I.U., Tian, B.H., Yong, L.I.U., Li, R.Q. and Xu, Q.Q. (2013) Hot Deformation Behavior and Processing Map of Cu-Ni-Si-P Alloy. *Transactions of Nonferrous Metals Society of China*, **23**, 2341-2347. [https://doi.org/10.1016/S1003-6326\(13\)62739-9](https://doi.org/10.1016/S1003-6326(13)62739-9)
- [8] Suzuki, S., Shibutani, N., Mimura, K., Isshiki, M. and Waseda, Y. (2006) Improvement in Strength and Electrical Conductivity of Cu-Ni-Si Alloys by Aging and Cold Rolling. *Journal of Alloys and Compounds*, **417**, 116-120. <https://doi.org/10.1016/j.jallcom.2005.09.037>
- [9] Naghash, A.R., Etsell, T.H. and Xu, S. (2006) XRD and XPS Study of Cu-Ni Interactions on Reduced Copper-Nickel-Aluminum Oxide Solid Solution Catalysts. *Chemistry of Materials*, **18**, 2480-2488. <https://doi.org/10.1021/cm051910o>
- [10] Syrett, B.C. (1981) The Mechanism of Accelerated Corrosion of Copper-Nickel Alloys in Sulphide-Polluted Seawater. *Corrosion Science*, **21**, 187-209. [https://doi.org/10.1016/0010-938X\(81\)90030-5](https://doi.org/10.1016/0010-938X(81)90030-5)
- [11] Gonçalves, R.S., Azambuja, D.S. and Lucho, A.M.S. (2002) Electrochemical Studies of Propargyl Alcohol as Corrosion Inhibitor for Nickel, Copper, and Copper/Nickel (55/45) Alloy. *Corrosion Science*, **44**, 467-479. [https://doi.org/10.1016/S0010-938X\(01\)00069-5](https://doi.org/10.1016/S0010-938X(01)00069-5)
- [12] Johansson, B.I., Lemons, J.E. and Hao, S.Q. (1989) Corrosion of Dental Copper, Nickel, and Gold Alloys in Artificial Saliva and Saline Solutions. *Dental Materials*, **5**, 324-328. [https://doi.org/10.1016/0109-5641\(89\)90124-3](https://doi.org/10.1016/0109-5641(89)90124-3)
- [13] Kear, G., Barker, B.D., Stokes, K.R. and Walsh, F.C. (2007) Electrochemistry of Non-Aged 90-10 Copper-Nickel Alloy (UNS C70610) as a Function of Fluid Flow: Part 1: Cathodic and Anodic Characteristics. *Electrochimica Acta*, **52**, 1889-1898. <https://doi.org/10.1016/j.electacta.2006.07.054>
- [14] Martinez, S. and Metikoš-Huković, M. (2006) The Inhibition of Copper-Nickel Alloy Corrosion under Controlled Hydrodynamic Condition in Seawater. *Journal of Applied Electrochemistry*, **36**, 1311-1315. <https://doi.org/10.1007/s10800-005-9101-z>
- [15] Metikoš-Huković, M., Babić, R., Škugor, I. and Grubač, Z. (2011) Copper-Nickel Alloys Modified with Thin Surface Films: Corrosion Behaviour in the Presence of Chloride Ions. *Corrosion Science*, **53**, 347-352. <https://doi.org/10.1016/j.corsci.2010.09.041>
- [16] Melchers, R.E. (2001) Temperature Effect on Seawater Immersion Corrosion of 90:10 Copper-Nickel Alloy. *Corrosion*, **57**, 440-451. <https://doi.org/10.5006/1.3290368>
- [17] El Din, A.S., El Dahshan, M.E. and El Din, A.T. (2000) Dissolution of Copper and Copper-Nickel Alloys in Aerated Dilute HCl Solutions. *Desalination*, **130**, 89-97. [https://doi.org/10.1016/S0011-9164\(00\)00077-1](https://doi.org/10.1016/S0011-9164(00)00077-1)
- [18] Schell, J., Heilmann, P. and Rigney, D.A. (1982) Friction and Wear of Cu-Ni Alloys. *Wear*, **75**, 205-220. [https://doi.org/10.1016/0043-1648\(82\)90149-1](https://doi.org/10.1016/0043-1648(82)90149-1)